International Journal for Scientific Research (IJSR)
المجلة الدولية للبحوث العلمية
Vol. (2), No. (9)
September 2023
الإصدار (2)، العدد (9)

Ultrathin Fe Films Sandwiched between Au Layers: CEMS- study

Mohamed M. Mohsen
Dept. of Biomedical Engineering, University of Tobruk, Libya
mohamed.mahmoud@tu.edu.ly

Moftah A. Hussain
Dept. of Biomedical Engineering, University of Tobruk, Libya
moftah.hussin@tu.edu.ly

Khalid S. Mustafa
Dept. of Laboratory Medicine, University of Tobruk, Libya
khalidshukri@yahoo.com

Mohammed T. Mostafa
Dept. of Laboratory Medicine, University of Tobruk, Libya
almesmoh@gmail.com

Abstract

The STM studies of Fe films with thickness above 0.6 ML do not contribute significantly to the solution of the structural problems, because of the Au surface layer, which hinders details of the Fe sub-surface layers. The Mossbauer spectroscopy appears in this case as an exceptional method, which has the ability to solve structural and magnetic problems. Our discussion is based on a simplified spectrum analysis, assuming a discrete character of the spectral components. In reality, a distribution of the hyperfine magnetic field, as well as isomer shift and the quadrupole splitting is an obvious and natural consequence of the finite size system 'presented by the monolayer film. The exact fitting of all hyperfine parameters distribution is too difficult. Most of the fitting procedures treat the distributions of IS

vs. Bhf and QS vs. Bhf as linearly dependent as described using the well-known Voigt-based method.

Keywords: Sandwich Structures, Magnetically Coupled Layers, Multilayered Systems, Monoatomic Superlattices.

1. Introduction

Through this paper, we ask what is Mössbauer spectrum analysis? While it is a versatile technology through which information can be improved in many disciplines such as physics, chemistry, and mineralogy. It can give very accurate information about structural, magnetic, and time-dependent morphology [15]. As for Mössbauer spectroscopy, it is a technique in which the interaction takes place between the electromagnetic moment of the nuclear charge and the electromagnetic field produced by the electrons outside the nucleus. This reaction gives nuclear splitting/transformation of energy levels.

New materials and ground states. The most common is the Van Mössbauer isotope, 57Fe, energy 5x10-9eV. Compare with Mössbauer gamma ray energy of 14.4 keV, which gives an accuracy of 1 in 1012 [16]. Mostly in transmission mode, the source is where the emission is: resonant gamma rays (free of backscatter), different from Gamma rays (which include bouncing), and therefore radiation from all other elements, so. The transformations are carried out by the production of secondary radiation (mainly X-rays) [17]. Therefore, it is necessary to study systems (mechanical, electromechanical, piezoelectric, hydraulic, etc.) constant speed and sweep speed systems [18]. Usually, the source is the one who makes the movement.

Up to 300 mm/s (1000 mm/c); Resonance frequency ~ 25 Hz, and in this case, we find that different modes allowed ~25 mm/s per volt. Detectors (scintillation detectors, proportional counters, germanium or silicon detectors drifting with

lithium). Proportional counter – Ar/Kr/Xe filled, ~2 kV operating voltage. You also need a lot of electronics, a cooling/oven system, ME installation software, and very precise parameters. The chemical isomer shift (IS) (δ): arises from the interaction between the nuclear charge density and the surrounding electron, chargecloud. The IS can provide information about the rotation status as well. Coordination number and quadrupole splitting (QS) (Δ): arises due to the interaction between the electric quadrupole moment of the nucleus and the electric field.

The resulting gradient is due to electrons. QS can provide information about the charge symmetry around the nucleus [19]. An ultrafine field gives the internal magnetic field. Isomer transformation as well as through Quadruple splitting where the ultrafine magnetic field also interacts with the magnetic dipole and electron quadrupole therefore, an idea of the magnetic moment can be obtained from the orientation of the "idealized" Mössbauer spectra [20, 21].

The STM studies of Fe films with thickness above 0.6 ML do not contribute significantly to the solution of the structural problems, because of the Au surface layer, which hinders details of the Fe sub-surface layers. The Mossbauer spectroscopy appears in this case as an exceptional method, which has the ability to solve structural and magnetic problems. There is no Mossbauer data in the literature, concerning ultra-thin Fe films grown on Au (001).

2. Methodology

2.1 Samples:

The choice of the samples was determined by two factors: (i) the sensitivity limit of CEMS does not allow it to go down below 1ML and (ii) films thicker than 5ML are nearly bulk as seen by CEMS. The interesting thickness range comprises then 1- 4 ML of Fe57. All The samples were grown on the standard reconstructed Au(001)hex

surface, which was used also for the STM studies. All films were prepared with the substrate held at about 300 K.

From the point of view of the LEED pattern symmetry, the four samples, with varying Fe thickness, from 1 to 4ML Fe, with the nominal thickness corresponding to full atomic layers, were similar. Fig.1 shows examples of LEED patterns for 1ML Fe (top) and 4ML Fe (bottom). A broadening of the LEED spots at the "out of phase" conditions (about 134eV), as shown in the profiles of the LEED pattern intensity for the 4ML Fe, is due to a random distribution of the pit-like structure, which was also seen on the STM pictures. Quantitative analysis shows that the monatomic roughness increases with increasing thickness, which could be an indication that the growth is not perfectly layer-by-layer. A deeper analysis of that problem based on the LEED or STM measurements is, however, difficult and indirect.

Figure 1. LEED patterns were observed for I ML Fe.

Not all CEMS measurements could be done in-situ and for the purpose of the ex-situ CEMS measurements, all samples were covered with a 3nm thick Au cap layer. The hex-type reconstruction is restored already after the completion of 2ML of the capping Au layer. It cannot be excluded that Fe layer is to some extent modified by

the Au overlayer. Therefore, the Fe films sandwiched between Au may not be compared directly with non-coated films, which have a single Au monolayer on top.

2.2 Room temperature CEMS measurements:

The overview of the CEMS spectra of Fe films with thickness varying from 1 to 4 ML is shown in Fig.2.The velocity scale refers to Co57(Rh) source which means that to obtain its isomer shift value against the metallic iron one must add 0.11 mm/s to the measured value.

The Curie temperature of the Fe monolayer lies below the room temperature. The observed doublet is due to a strong quadrupole interaction, whose source might be the lack of translational symmetry but also a deviation from the cubic symmetry. The interpretation of the monolayer spectrum is one of the essential problems of this paper. All samples above one monolayer are magnetically split at room temperature. They show a rather distinct six-line Zeeman pattern, with a certain amount of a low field (or non-magnetic) component only for the 2 ML sample. This is the first rough indication that the Fe atoms embedded in the Au matrix form really flat films, with sharp interfaces and no pronounced intermixing with Au atoms.

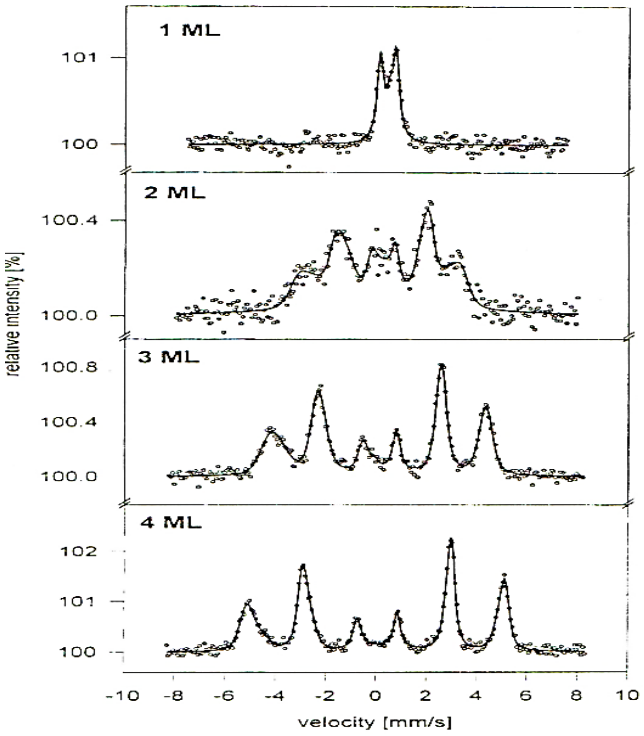

Figure 2. The RT CEMS spectra of Fe films with thickness varying from 1 to 4 ML.

The magnetic spectra were analyzed by fitting a hyperfine field distribution (HFD) using the Voigt-based method of Rancourt and Ping [1]. In this method, a convolution of the Mossbauer Lorentzian sextets with Gaussian distributions is used to fit the spectrum. Up to five generalized sites, represented by different IS vs. Bhf and QS vs. Bhf correlations can be defined. The HFD for the given site is approximated by a sum of up to five Gaussian components. The method is particularly useful in the case of ill spectrum statistics and allows in this case to determine reliably average parameters and the most typical and distinct features in HFD. The results of the fits, represented by the solid lines in Fig.2, are summarized in Fig.3 and in Table 1.

The distribution of the magnetic hyperfine fields (Fig.3.a) is systematically shifted toward the lower field and broadened by decreasing the film thickness. The mean value of the Bhf (Fig.3.b) saturates rapidly for thicker films and for the 4ML film reaches nearly the bulk value. The observed dependence of <Bhf-> on the temperature is mainly due to the thickness variation of the Curie temperature Tc. The determination of the Tc for ultra-thin films presents a difficult and challenging problem. It has been solved for certain monolayer systems when the Tc does not exceed the room temperature, and the temperature cycles do not change the film structure [2].

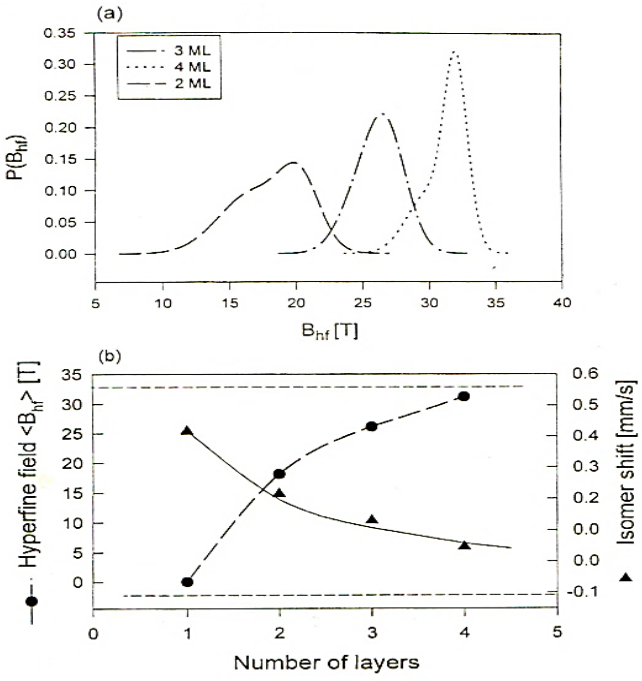

Figure 3. The distributions of the hyperfine magnetic field for 2-4ML Fe films (a\0, the thickness dependence of average hyperfine magnetic field $<B_{hf}>$, and isomer shift IS (b).

Table 1. below shows the average hyperfine interaction parameters, separately for the magnetic and non-magnetic components in the RT CEMS spectra of ultra-thin Fe film, obtained from Voigt-based fit of HFD distribution. Numbers in parentheses denote the uncertainty of the last digit. IS is given against the Co57(Rh)source.

Table 1.

Film thickness [ML]		<B_{hf} [T]>	<IS> [mm/s]	<QS> [mm/s]	Relative contribution
1	Magnetic	18.1(2)	0.216(5)	-0.05(2)	0.69(2)
	Non-magnetic	---	0.40 (1)	0.18(5)	0.31(2)
2	Magnetic	26.1(1)	0.131(2)	-0.02(1)	0.94(1)
	Non-magnetic		0.305(5)	0.4(1)	0.06(1)
3	Magnetic	3 1 .2(1)	0.047(1)	0.006(5)	0.47(2)
	Non-magnetic	---	---	---	not observed

From the present studies, due to the strong thickness dependence of the Bhf on the film thickness, TC can be roughly estimated without temperature measurements. As a guideline for the TC estimation, it is assumed that the dependence of the reduced <Bhf> value <Bhf(T/TC)> = <Bhf(T/TC)>/Bhf(0) versus the reduced temperature falls between two curves, as shown schematically in Fig.4. Curve (a) represents the bulk-like behavior, whereas the linear dependence (b) sets the limit of the fastest magnetization reduction expected for a 2-D spin-wave behavior. In fact, for continuous films, which are free from superparamagnetic effects, the mean-field theory for spin 1/2 (a) is also a good approximation of the 2-dimensional behavior, if one excludes the critical region [3]. Setting an arbitrary ground state value of Bhf as 35T the <Bhf)> value can be located in Fig.4, as shown by the dotted lines. This

rough estimation gives the TC values not lower than 330K, 400K, and 500K for 2, 3, and 4 monolayer films, respectively.

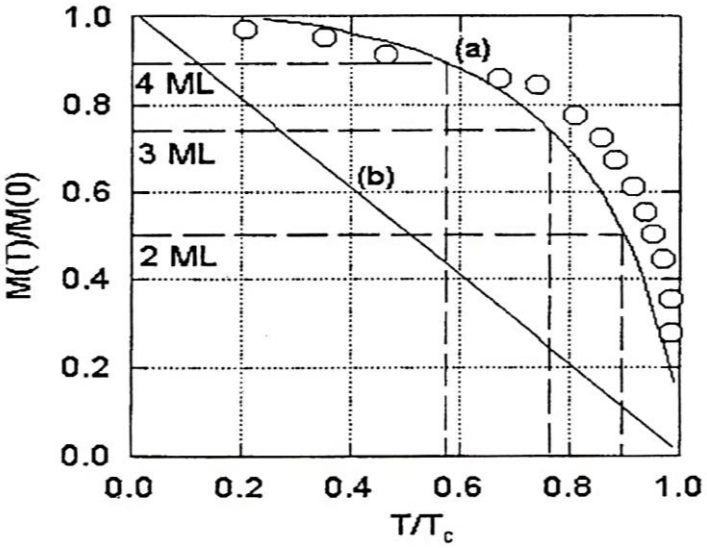

Figure 4. The reduced magnetization versus reduced temperature curves for the bulk-like behavior (a), and for 2D spin-wave behavior (b)

The prediction coincides well with a rather general observation that TC is reduced to half of its bulk value (1043 K for Fe) at a thickness of about five monolayers. The average isomer shift, also shown in approaches to the bulk value (-0.11mm/s against the Co57(Rh) source) is much slower than the hyperfine magnetic field. It reflects different mechanisms, which are responsible for both physical quantities. In the case of Bhf, the collective character of magnetic order dominates over the details of the electronic structure at the interfaces [4]. It implies a fast exponential decay of the size effect. The thickness modification of the isomer shift comes from the very interface, because of the strong screening mechanism in metals. The resulting value of the <IS> is the weighted average from the interface and the film interior. <IS>

scales as one over the film thickness (the solid line in Fig.3.b), yielding 1.5 ML as the thickness of the interface which is affected by the influence of Au.

For all magnetic spectra, the intensity ratio of the lines in the sextet is 3:4:1. For the given experimental geometry, it means that spontaneous magnetization lies in the film plane. For ultra-thin Fe(001) films on gold, the perpendicular magnetization was observed even for films as thick as 3 monolayers [5], but the anisotropy was always found to be very sensitive to the preparation condition and the annealing [6]. The magnetic anisotropy of the films will be discussed in comparison with multilayers.

2.3 Monolayer film:

The Curie temperature for the 1 ML film is below room temperature. The CEMS spectrum at room temperature is represented by the asymmetric doublet as shown in Fig 2. The spectrum was measured also with the lower velocity scale, showing a more complicated structure. The CEMS spectrum measurements in the monolayer range are very time-consuming and it was not possible to perform the CEMS measurements in a wide temperature range. The 80 K monolayer spectrum, shown in Fig 5 had to be measured for two weeks, despite the extremely strong source (200 mCi). Already by a visual inspection, the spectrum shows certain unusual features not observed for the thicker films. It is highly asymmetric, the sextet-like structure is difficult to identify, and the intensity ratio differs from one expected for the in-plane magnetization.

There is also an abnormally deep level close to zero velocity, which is an experimental artifact. It comes from the resonant absorption in the Al foil, used in the CEMS chamber to filtrate X-rays, which contains traces of iron. For the resonant effect exceeding 1%, the effect of the foil is lower than spectral noises, but for the monolayer giving the effect of 0.3 %, it becomes significant and must be considered in the numerical analysis.

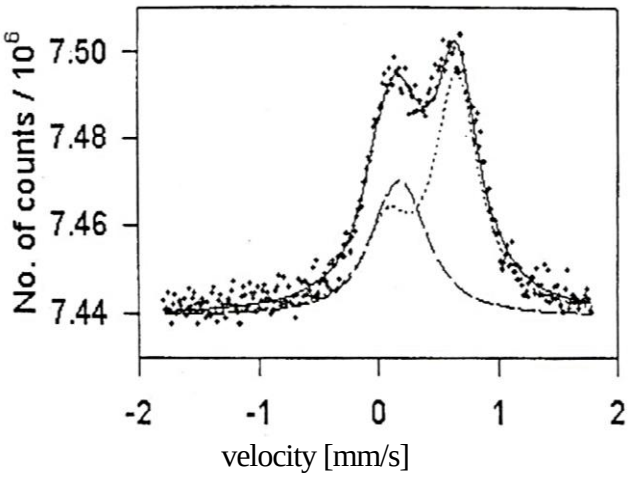

Figure 5. RT CEMS spectrum for 1 ML Fe film measured with the lower velocity scale. The best fit consisting of the two components (single line — dashed line, quadruple doublet — dotted line) is also included.

A first approximation of the spectrum interpretation can be obtained by a fit with discrete Zeeman components. Obviously, there is a pronounced line-broadening going toward higher velocities due to the distribution of a hyperfine parameter, which has to be taken into account by a fit. It can be done by introducing different values of the Mossbauer line half-width F for different Mossbauer transitions, the widths being constrained according to the formula [7].

$$\Gamma = \Gamma_0 + \left(\frac{4\delta B_{hf}}{\Gamma_0}\right) * < B_{hf} >^2 * \alpha^2,$$

where r 0 is the natural half width of the Mossbauer line 613hf and <Bhf> are the width and the mean value of the Bhf distribution, respectively, and a = ggNmg -

gexNmex depends on the transition. The procedure does not take into account isomer shift and quadrupole splitting distribution but gives approximate positions of the maxima in the Bhf distribution. The fit with three discrete components and its interpretation is shown in Fig.6 and Table 2. The negative intensity component (single line) is related to the resonant absorption in the Al foil used in the CEMS setup to filtrate X-rays. Following the interpretation of the spectra for the thicker films, the isomer shift value can be treated as a "fingerprint", which identifies the configuration of Fe atoms.

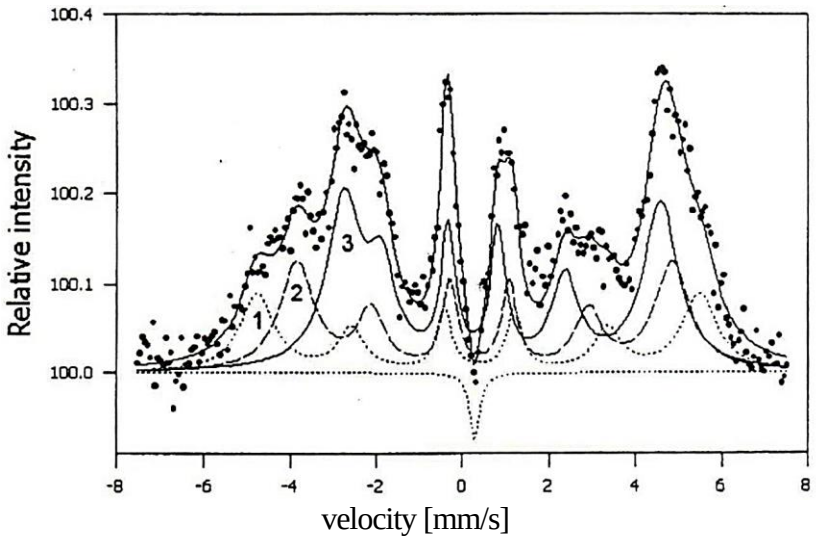

Figure 6. The 80 K CEMS spectrum for the Fe monolayer with the best fit is presented. The three discrete components "1", "2", & "3", are due to a triple, double, and a monolayer, respectively.

Remembering the STM studies it is reasonable to assume that during the monolayer growth the deviation from a perfect layer-by —layer growth may result in monolayer patches or double and triple Fe layers. Accordingly, the components "1", "2" and "3" are interpreted as coming from a triple layer, a double layer, and a monolayer,

respectively. It follows not only from the isomer shift. Not only the isomer shift but also the quadrupole splitting, and hyperfine magnetic field support such interpretation. The monolayer component has the hyperfine interaction parameters strongly deviating from bulk. The most striking is the large quadrupole interaction of 0.34 mm/s. A non-zero quadrupole interaction, which appears at surfaces or interfaces, is a typical consequence of the broken translational symmetry, as it was proved by PAC and Mossbauer measurements. For example, for the Fe(110)/Ag interface, the quadrupole splitting of about 0.1 mm/s could be interpreted in terms of electrostatic effects at the interfaces [8]. The presently reported value is that much higher, that structural effects should be involved in its interpretation. Certainly, the local symmetry of the Fe atoms in a monolayer is reduced and the most probable explanation is a tetragonal distortion that accompanies the epitaxial growth of Fe on Au.

Table 2. Average hyperfine interaction parameters for 1ML Fe film at 80 K, were obtained from a discrete fit. Numbers in parentheses denote the uncertainty of the last digit. IS is given against the Co57 (Rh) source.

Table 2.

Spectral component	Bhf [T]	IS [mm/s]	QS [mm/s]	Relative contribution
1	31.9(2)	0.37(1)	-0.02(1)	0.22(2)
2	27.1(2)	0.45(1)	0.06(1)	0.31(2)
3	22.84(9)	0.581(7)	0.3379(9)	0.47(2)

One of the most important results is the determination of the monolayer magnetic hyperfine field, which was found as 22.8 T at 80 K. The ground state value is however not sure, because the Curie temperature of the monolayer is unknown. Nevertheless, because the triple layer Bhf from the same spectrum is only by about

10% lower than the ground state value, (25±1) T is a reasonable estimation of the monolayer ground state Bhf value. The electronic and magnetic properties of the Fe/Au (001) system were calculated by Li et al. [9] and Guo and Ebert [10]. The calculated system presents a pretty good structural match to the real structure, which is a rather seldom case when an experiment on epitaxial magnetic films is compared with a theory. Li et al. calculated the properties of a Fe monolayer represented by a single-slab geometry with one layer of p(lx1) Fe on both sides of a five-layer Au slab, without taking into account a relaxation and reconstruction. They calculated only the contact hyperfine magnetic field. They obtained the total value of the field -21.3T, composed of the negative core electron contribution (-41.4 T) and very large positive conduction electron term 20.0 T. The total field, considerably reduced compared to the bulk, does not scale with the magnetic moment, which is strongly enhanced (2.97 t5). Considering discrepancies between the experimental and theoretical systems (the main one is that in the calculation the monolayer is uncoated), the calculated Bhf agrees reasonably with the experimental value.

It is worth noting, that the reduction of the monolayer Bhf contradicts the tendency at the Fe/Au interface, where an increase in the hyperfine magnetic field was observed [11]. In this respect, the reported case is the first ever-reported experimental evidence of the strong Bhf suppression in Fe monolayer on a simple metal. The Mossbauer data concerning an iron monolayer are available for Fe on a d-metal (W(110) and Cr(110) and on a noble metal (Ag(001) and Ag(111) [12, 13]. The reduction of the monolayer Bhf for Fe on d-metals coincides with the reduction of the interface Bhf value in these systems and it is intuitively expected. For a monolayer on a noble metal, only an enhancement of Bfh was found, contradicting the theory. It was probably caused by a three-dimensional Fe growth, hindering the observation of a true monolayer. The present studies removed then the long-lasting controversy between the experiment and the theory.

Guo and Ebert calculated magnetic moment and magnetic hyperfine fields in a [1ML Fe bcc(001)/5 ML Au fcc (001)] multilayer, which presents a very good approximation of the Fe monolayer, at least when ground state properties are concerned [10]. In their calculation, not only the contribution to the hyperfine fields due to the conventional Fermi contact interaction but also due to the spin-orbital and orbital contribution induced by the crystal field and by spin-orbit coupling are accounted for. They found a very pronounced anisotropy of the hyperfine field determined by calculations for in plane and perpendicular anisotropy, very closely connected with the corresponding anisotropy of the magnetic dipole moment and the orbital moment. They calculated Bhf=-22.4 T for the in-plane moments and Bhf= -17.0T for perpendicular ones, without however stating which situation is energetically more favorable. It is also obvious that any symmetry modification (e.g a relaxation of the Au-Fe interlayer spacing leading to a tetragonal distortion) can modify the anisotropic Bhf contributions largely.

The problem of the magnetic anisotropy in the Fe monolayer on Au(001) is addressed also in the paper by Okabayashi, Jun, et al [14], that the anisotropies are not sensitive to changes in the structural parameters of a few percent. The calculations for the Fe monolayer sandwiched between Au(001) are lacking. The line intensity ratio of the Mossbauer sextet is 3:1.25:1, which is very close to the theoretical ratio of 3:1.33:1 expected for the experimental geometry for the perpendicular magnetization. The magnetization switching from an in-plane to the normal direction, which is observed only for the monolayer film, may be connected with the tetragonal distortion postulated for the explanation of the large quadrupole splitting. The lowering of the symmetry accounts for the modification of the spin-orbit coupling because the orbital moment quenching is not complete. Based on the relative contribution of the spectral components, which were identified as coming from a monolayer, a double layer, and a triple layer, a model of a solid-on-solid-like film can be constructed as shown in

Fig. 7. The nominal 1 M1 of Fe is distributed over the three atomic layers: in the first one 70% of Fe atoms, is deposited 23 % in the second one and only 7% in the third one, confirming a growth mode not far from the ideal layer by layer.

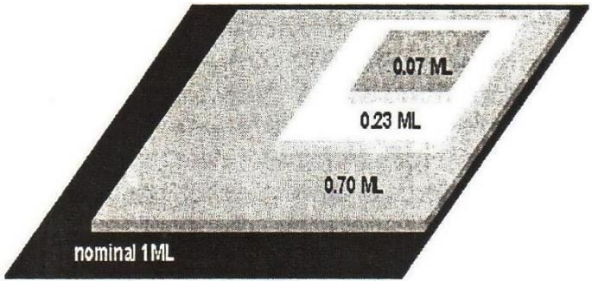

Figure 7. Model of a solid on solid-like film, based on the relative contribution of the spectral components resulting from the Fe monolayer 80K CEMS spectrum fit.

3. Results and Discussion

The discussion above is based on a simplified spectrum analysis, assuming a discrete character of the spectral components. In reality, a distribution of the hyperfine magnetic field, as well as isomer shift and the quadrupole splitting is an obvious and natural consequence of the finite size system presented by the monolayer film. The exact fitting of all hyperfine parameters' distribution is too difficult. Most of the fitting procedures treat the distributions of IS vs. Bhf and QS vs. Bhf as linearly dependent as it was described for Voigt-based method. The additional problem for the monolayer film comes from the large quadrupole interaction, which is on the limit of the applicability of the formulas for the energy splitting when the magnetic interaction dominates over the quadrupole one. It is also possible that the QS vs. Bhf correlation obtained from a fit is systematically erroneous, because in the effective Hamiltonian. Only the product of the angular factor, V,, and n is essential and different combination of the quadrupole interaction parameters may result in the same set of the hyperfine levels. In spite of the above considerations, the 80 K

monolayer spectrum was also fitted with a distribution method. A Voigt-based program has a limitation of the site number and therefore so-called Le Caer program was used [13], in which a quasi-continuous distribution is fitted. The results of the fit are shown in Fig.8.

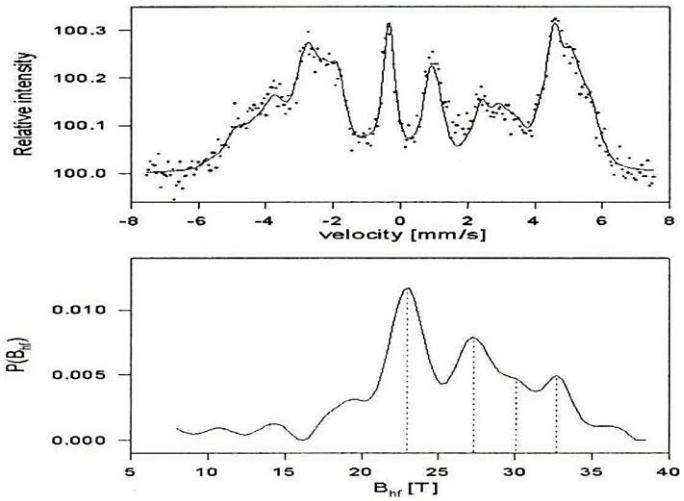

Fig. 8. The 80 K monolayer spectrum fitted with the quasi-continuous hyperfine magnetic field distribution method, and, resulting Bhf distribution.

The single absorption line from Al foil was subtracted from the spectrum in Fig.8.a. The magnetic hyperfine field distribution presented in Fig.8.b reveals additional details as compared with the previous fit but the main features of the Bhf distributions agree with the discrete components. The monolayer peak at 23T is the most distinct and narrow feature. The bulk-like peak at about 33T is also well resolved, whereas the maxima between 25 T and 30 T are rather broad. Apparently, according to the growth model shown in Fig. 7, double-layer areas, represented by the field between 25 T and 30 T are most sensitive to the local Fe configuration. It seems also that all Fe atoms at steps and other linear defects, with a reduced number of magnetic nearest neighbors, contribute to that broad component.

Fig. 9 compares the IS vs. Bhf and QS vs. Bhf correlation obtained from the discrete fit (points) and HFD fit. For the IS the linear correlation imposed by the HFD fit holds quite well, but for the quadrupole interaction, a stronger dependence should be used. Alternatively, a fitting procedure allowing different sites with various correlations must be applied.

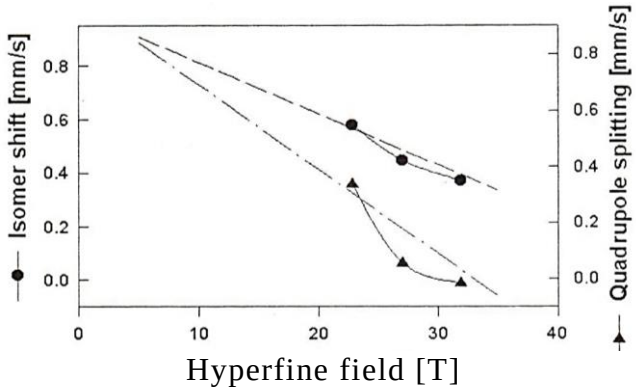

Figure 9 Comparison of the IS vs Bhf, and QS vs Bhf correlations obtained from the discrete fit (points) and HFD fit (lines) of the 80K monolayer spectrum.

Conclusion

In this work, it is found that the finite size of the STM studies systems shows a discreet character of spectral components such behavior appears in the distribution of hyperfine magnetic field as well as isomer shift and quadruple splitting. An additional problem is the large quadruple interactions that are over the range of the formulas applied for energy splitting when the magnetic interaction demonstrates over quadruple one.

Through this research, we recommend studying this system in more depth and comparing materials in order to determine the reason for the ineffectiveness of the Hamiltonian of the monoatomic system.

References

1. Rancourt, D. G., and J. Y. Ping. "Voigt-based distributions methods for arbitrary-shape in Mössbauer spectroscopy static hyperfine parameter." *Nucl. Instrum. Methods Phys. Res. B* 58 (1991): 85-97.
2. Suwa, Tomomi, Satoshi Tomita, Nobuyoshi Hosoito, and Hisao Yanagi. "Magnetic properties of fibonacci-modulated Fe-Au multilayer metamaterials." *Materials* 10, no. 10 (2017): 1209.
3. Takahashi, Y., T. Miyamachi, S. Nakashima, N. Kawamura, Y. Takagi, M. Uozumi, V. N. Antonov, T. Yokoyama, A. Ernst, and F. Komori. "Thickness-dependent electronic and magnetic properties of γ′− Fe 4 N atomic layers on Cu (001)." *Physical Review B* 95, no. 22 (2017): 224417
4. Muratov, Cyrill B., and Valeriy V. Slastikov. "Domain structure of ultrathin ferromagnetic elements in the presence of Dzyaloshinskii–Moriya interaction." *Proceedings of the Royal Society A: Mathematical, Physical and Engineering Sciences* 473, no. 2197 (2017): 20160666.
5. Yuan, Jiangtan, Andrew Balk, Hua Guo, Qiyi Fang, Sahil Patel, Xuanhan Zhao, Tanguy Terlier, Douglas Natelson, Scott Crooker, and Jun Lou. "Room-temperature magnetic order in air-stable ultrathin iron oxide." *Nano letters* 19, no. 6 (2019): 3777-3781.
6. An, Li, Jianrui Feng, Yu Zhang, Yong-Qing Zhao, Rui Si, Gui-Chang Wang, Fangyi Cheng, Pinxian Xi, and Shouheng Sun. "Controllable tuning of Fe-N nanosheets by Co substitution for enhanced oxygen evolution reaction." *Nano Energy* 57 (2019): 644-652
7. Martel, Laura, Amir Hen, Yo Tokunaga, François Kinnart, Nicola Magnani, Eric Colineau, Jean-Christophe Griveau, and Roberto Caciuffo. "Magnetization, specific heat, O 17 NMR, and Np 237 Mössbauer study of U 0.15 N p 0.85 O 2." *Physical Review B* 98, no. 1 (2018): 014410.
8. Mitsui, T., S. Sakai, S. Li, T. Ueno, T. Watanuki, Y. Kobayashi, R. Masuda, M. Seto, and H. Akai. "Magnetic Friedel Oscillation at the Fe (001) Surface: Direct Observation by Atomic-Layer-Resolved Synchrotron Radiation Fe 57 Mössbauer Spectroscopy." *Physical Review Letters* 125, no. 23 (2020): 236806.
9. Li, Chun, A. J. Freeman, and C. L. Fu. "Monolayer magnetism: electronic and magnetic properties of Fe/Au (001)." *Journal of magnetism and magnetic materials* 75, no. 3 (1988): 201-208.
10. Guo, G. Y., and H. Ebert. "First-principles studies of the magnetic hyperfine field in Fe multilayers." *Hyperfine interactions* 97, no. 1 (1996): 11-18.

11. Ślęzak, M., T. Ślęzak, K. Freindl, W. Karaś, N. Spiridis, M. Zając, A. I. Chumakov, S. Stankov, R. Rüffer, and J. Korecki. "Perpendicular magnetic anisotropy and noncollinear magnetic structure in ultrathin Fe films on W (110)." *Physical Review B* 87, no. 13 (2013): 134411.
12. Kiss, L. F., J. Balogh, L. Bujdosó, and D. Kaptás. "Magnetic properties of Fe-Ag multilayers with varying layer thickness and bilayer number." *Physical Review B* 98, no. 14 (2018): 144423.
13. Le Caër, G., and J. M. Dubois. "Evaluation of hyperfine parameter distributions from overlapped Mossbauer spectra of amorphous alloys." *Journal of Physics E: Scientific Instruments* 12, no. 11 (1979): 1083.
14. Okabayashi, Jun, Songtian Li, Seiji Sakai, Yasuhiro Kobayashi, Takaya Mitsui, Kiyohisa Tanaka, Yoshio Miura, and Seiji Mitani. "Perpendicular magnetic anisotropy at the Fe/Au (111) interface studied by Mössbauer, x-ray absorption, and photoemission spectroscopies." *Physical Review B* 103, no. 10 (2021): 104435.
15. Mössbauer Spectroscopy and its Applications, T E Cranshaw, B W Dale, G O Longworth and C E Johnson, (Cambridge Univ. Press: Cambridge) 1985.
16. Mössbauer Spectroscopy, D P E Dickson and F J Berry, (Cambridge Univ. Press, 1986.
17. The Mössbauer Effect, H Frauenfelder, (Benjamin: New York) 1962.
18. Principles of Mössbauer Spectroscopy, T C Gibb, (Chapman and Hall: London) 1977.
19. Mössbauer Spectroscopy, N N Greenwood and T C Gibb, (Chapman and Hall: Novel Materials and Ground States London), 1971.
20. Chemical Applications of Mössbauer Spectroscopy, V I Goldanskii and R H Herber ed., (Academic Press Inc: London) 1968.
21. Mössbauer Spectroscopy Applied to Inorganic Chemistry Vols. 1-3, G J Long, ed., (Plenum: New York) 1984-1989.
22. 21. Mössbauer Spectroscopy Applied to Magnetism and Materials Science Vol. 1, G J Long and F Grandjean, eds., (Plenum: New York) 1993.